SUPPLEMENTARY MATERIAL

Title: Strong FGFR3 staining is a marker for *FGFR3* fusions in diffuse gliomas

Authors: Kirsi J. Granberg, Matti Annala, Birgitta Lehtinen, Juha Kesseli, Joonas Haapasalo, Pekka Ruusuvuori, Olli Yli-Harja, Tapio Visakorpi, Hannu Haapasalo, Matti Nykter, Wei Zhang

Supplementary Table 1. Demographic, clinical and therapy information about the patients in the astrocytoma cohort that was used in cause-specific survival analysis. All are primary tumor samples that have been obtained from tumor surgery patients at Tampere University Hospital between 1983 and 2009. Patient age and follow-up information are shown in Table 1. The tumors were radically resected when possible. Detailed information about different oncological therapy modalities for grade II-IV astrocytoma patients at Tampere University Hospital was available from the time period 2002-2009. Temozolomide has been in use at the hospital since year 2002. Patients that received radiation-chemotherapy are also included into the radiotherapy- and chemotherapy-treated patient cohorts.

	Number of patients	
Sex		
Male	316	
Female	214	
Tumor grade		
II	80	
III	41	
IV	409	
Therapy	**Treated**	**Total**
Radiotherapy	131	173
Chemotherapy	100	183
Radiation-chemotherapy	70	150

Supplementary Table 2. Target regions for probe design for targeted sequencing. Coordinates were extracted using genome assembly GRCh37/hg19.

Genomic region	Target
chr4:1,790,039-1,820,600	FGFR3 locus
chr8:38,258,656-38,331,352	FGFR1 locus
chr5:1,295,162-1,295,662	TERT promoter (500 bp)
chr13:48,877,883-49,056,026	RB1 exons
chr21:17,911,328-17,911,570	miR-99a locus
chr9:8,314,246-10,612,723	PTPRD exons
chrX:76,937,000-76,940,142	ATRX # exon 8
chrX: 76,763,788-76,891,418	ATRX # exons 16-end
chr8:38,585,704-38,710,546	TACC1 exons
chr4:1,723,217-1,746,905	TACC3 exons
chr9:21,967,751-21,994,490	CDKN2A exons
chr10:89,623,195-89,728,532	PTEN exons
chr3:178,916,614-178,952,152	PIK3CA exons in coding region
chr12:112,856,536-112,947,717	PTPN11 exons
chr4:55,095,264-55,146,925	PDGFRA exons
chr4:55,095,264-55,146,925	MET exons
chr17:7579650-7579750	TP53 # exon 3
chr17:7579300-7579600	TP53 # exon 4
chr17:7578350-7578570	TP53 # exon 5
chr17:7578150-7578300	TP53 # exon 6
chr17:7577480-7577630	TP53 # exon 7
chr17:7577000-7577180	TP53 # exon 8
chr17:7576840-7576940	TP53 # exon 9
chr17:7576520-7576680	TP53 # exon 10
chr17:7573910-7574050	TP53 # exon 11
chr2:209113040-209113190	IDH1 # exon 4
chr15:90631790-90631940	IDH2 # exon 4
chr11:65429530-65431330	RELA # exons 1-3
chr7:140453090-140453190	BRAF # exon 15
chr7:140481400-140494300	BRAF # exons 8-11
chr7:55084974-55275667	EGFR gene
chr5: 60003061 -80002241	CNA negative control region 1 (21 probes)
chr8: 60001061 -80002241	CNA negative control region 2 (21 probes)
chr18: 30000975 -50001334	CNA negative control region 3 (14 probes)
chr11: 70001061-90005243	CNA negative control region 4 (19 probes)

Supplementary Table 3. FGFR3 staining was associated with poor cause-specific survival in astrocytoma (n = 301). A COX regression analysis included IDH1 mutation (based on IDH1 p.R132H IHC staining), patient age, tumor proliferation index (based on Ki-67 IHC staining), tumor grade, and FGFR3 IHC staining as explanatory factors. RR: relative risk, CI: confidence interval.

Risk factor	RR	95 % CI	p-value
IDH1 mutation	0.316	0.212-0.471	<0.001
Age	1.624	1.362-1.938	<0.001
Proliferation index	1.404	1.202-1.639	<0.001
Grade	1.344	1.048-1.725	0.020
FGFR3	1.296	1.010-1.666	0.042

Supplementary Table 4. Overview of genetic alterations observed in FGFR3-fusion positive cases (separate file)

Supplementary Table 5. Mutations detected in targeted sequencing cohort (separate file)
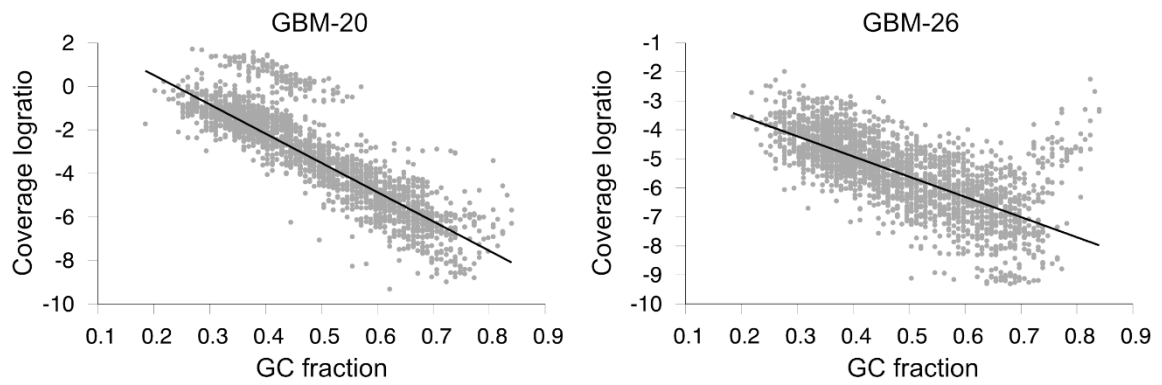
Supplementary Figure 1. Two examples showing the linear relationship between GC content and coverage logratio bias.
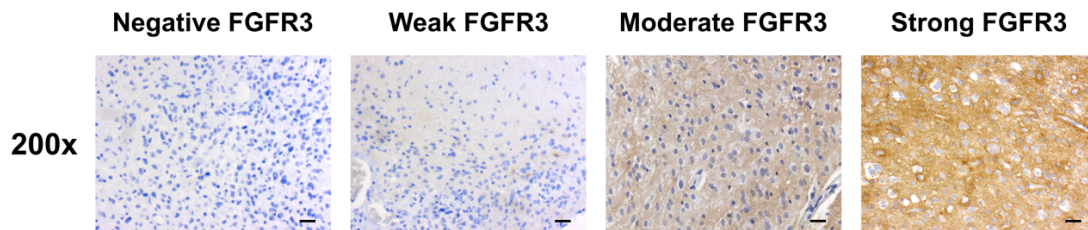
Supplementary Figure 2. Representative staining images in oligodenroglial samples. Scale bar 20 μm.

a)
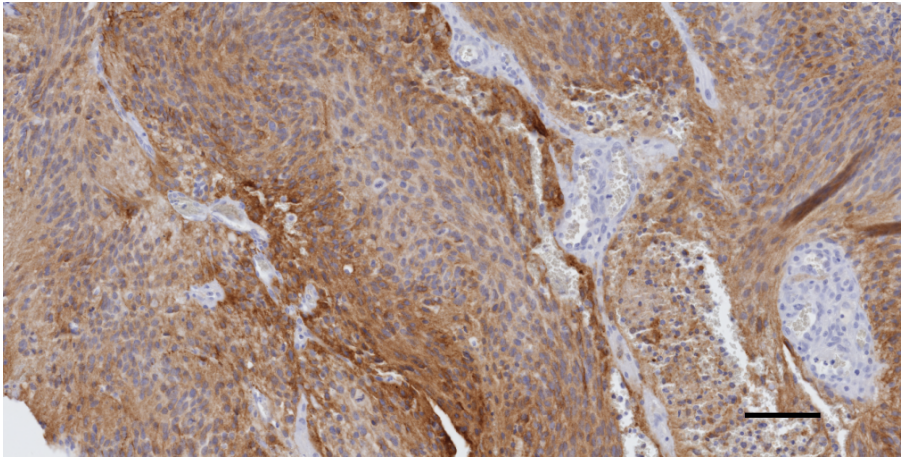
b)
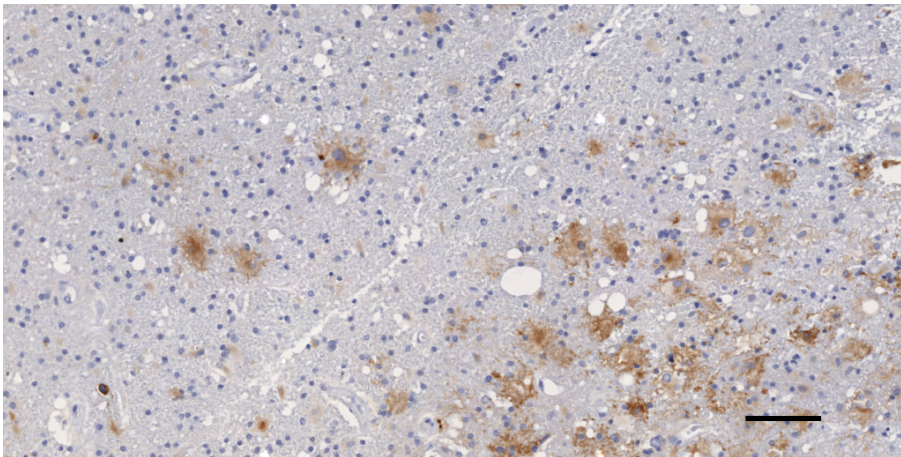
c)
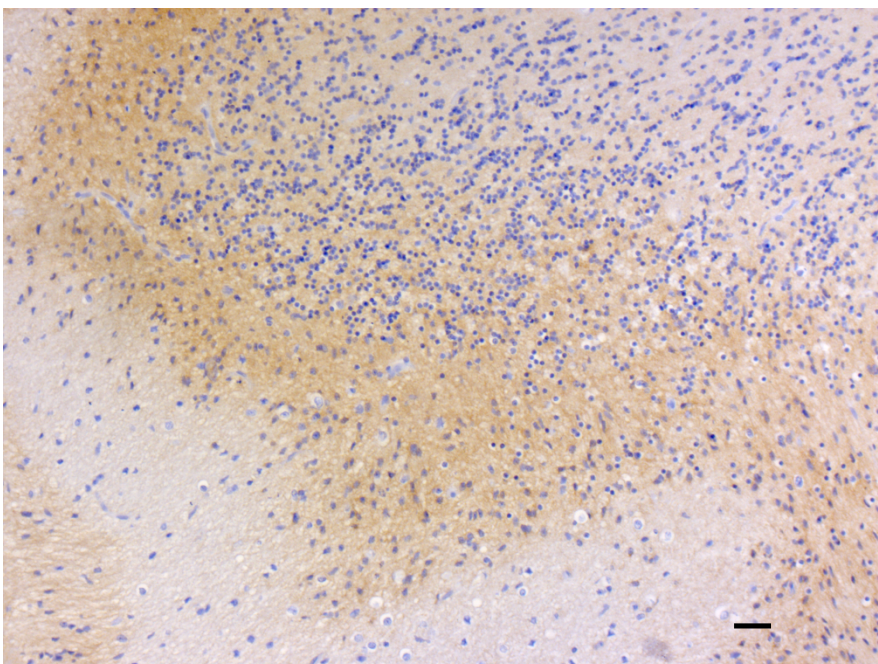
Supplementary Figure 3. a) Blood vessels stain negative with FGFR3 antibody (100x magnification, scanned images). b) Representative image showing negative staining in normal brain and positive staining in infiltrating tumor cells (100x magnification, scanned images). c) Weak-to-moderate FGFR3 staining was observed in cerebellar molecular layer (100x magnification, camera image). Scale bar 25 μm in all the images.
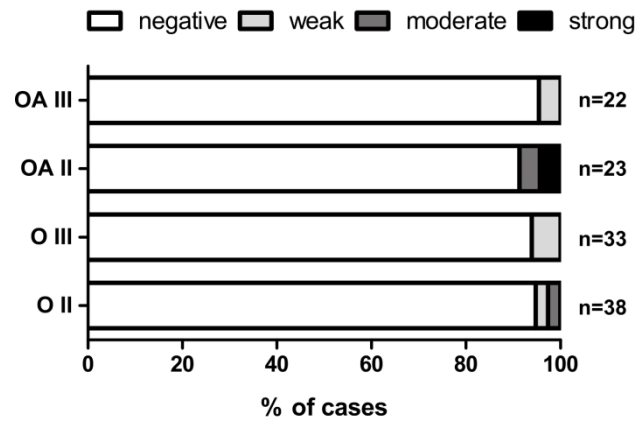
Supplementary Figure 4. FGFR3 staining distribution in oligodendroglial tumors. O II: grade II oligoastrocytoma, O III: grade III anaplastic oligodendroglioma, OA II: grade II oligoastrocytoma, OA III: grade III anaplastic oligoastrocytoma.

Supplementary Figure 5. Association analyses in astrocytoma cohort. p-values were calculated using Fisher's exact test. Cut-off points for patient age classes were 20, 40, 60, and 80 years. In FGFR1 and FGFR3 class, cases were separated into positive (moderate or strong staining) and negative (negative or weak staining) classes. Oper: primary or recurrent tumor, p53: p53 IHC staining, idh: IHD1 p.R132H mutation staining.
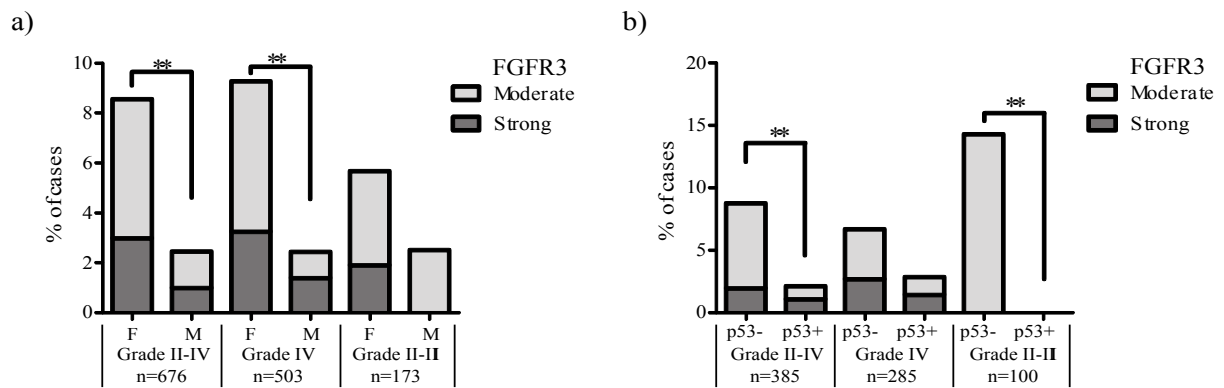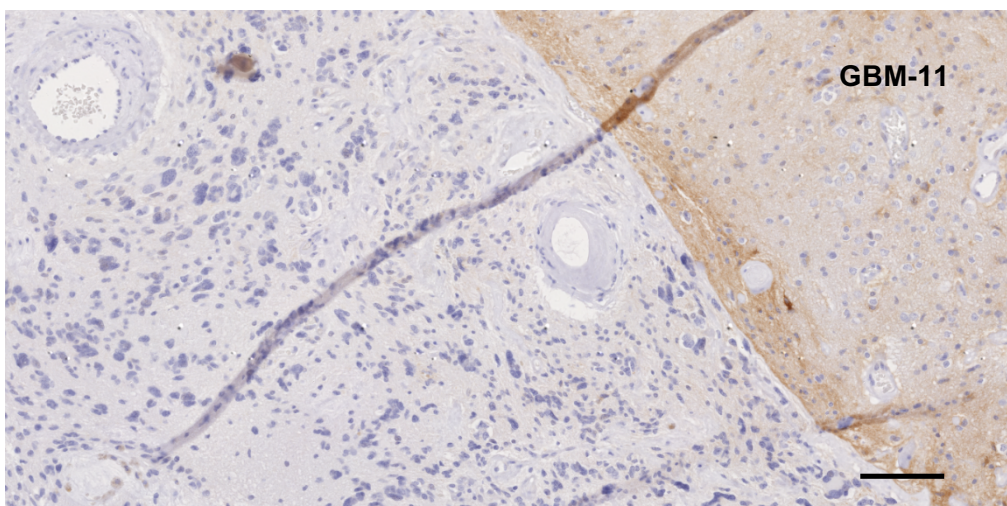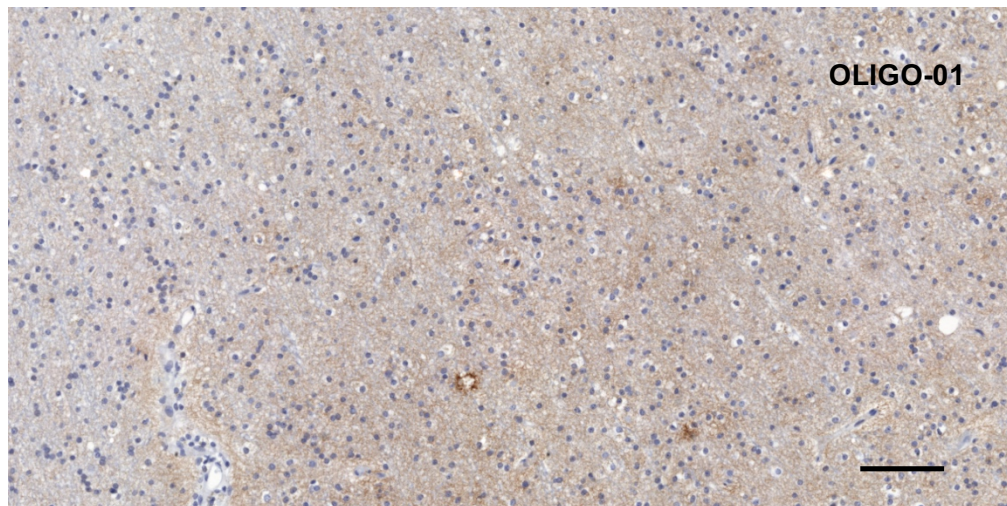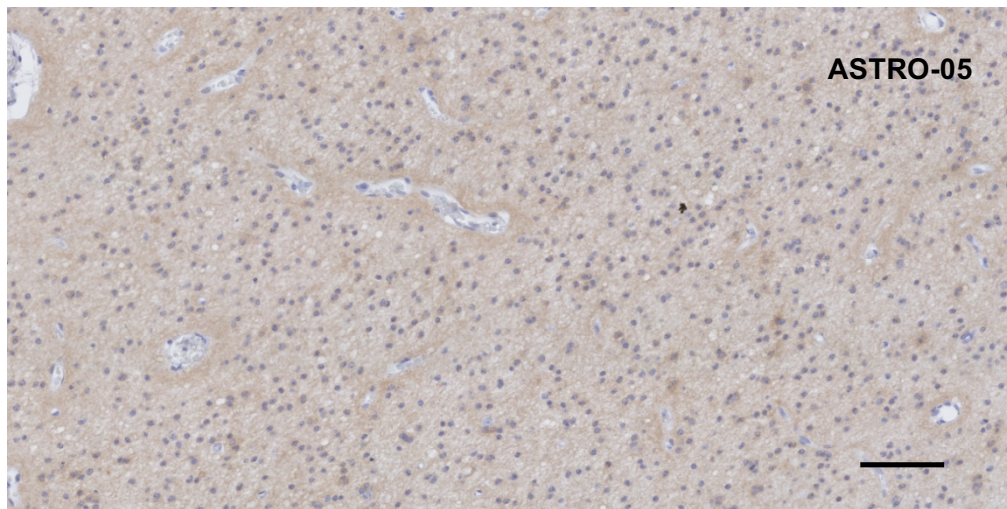
Supplementary Figure 6. Moderate-to-strong FGFR3 staining was associated with patient sex and p53 status in diffuse astrocytoma. a) Moderate-to-strong FGFR3 staining was more common in females than in males. ** p< 0.01, Fisher's exact test. b) Moderate-to-strong FGFR3 staining was negatively associated with aberrant p53 expression (>5% of cells with positive staining). In grades II-III, they were mutually exclusive. ** p < 0.01, Fisher's exact test.
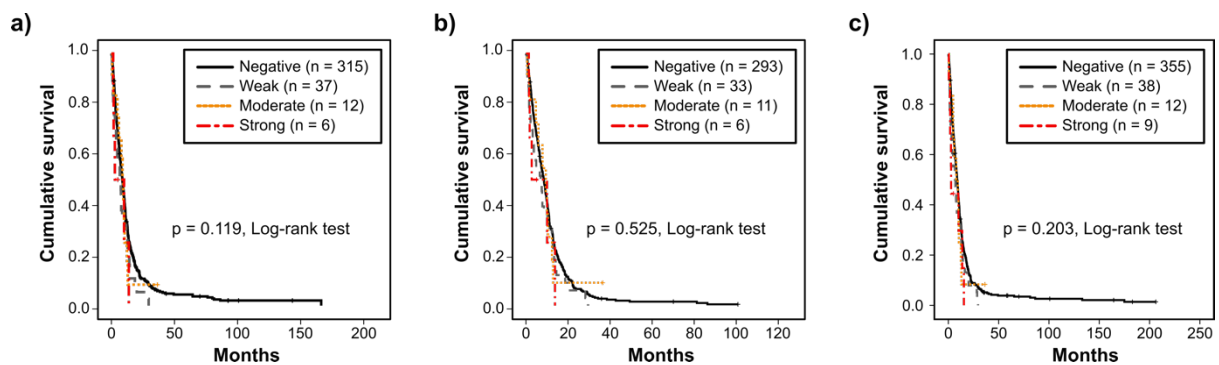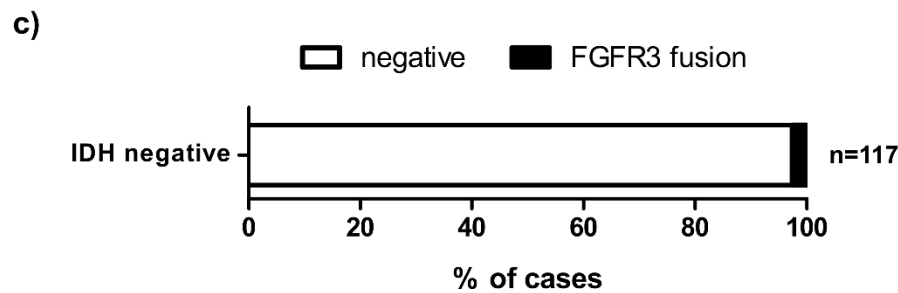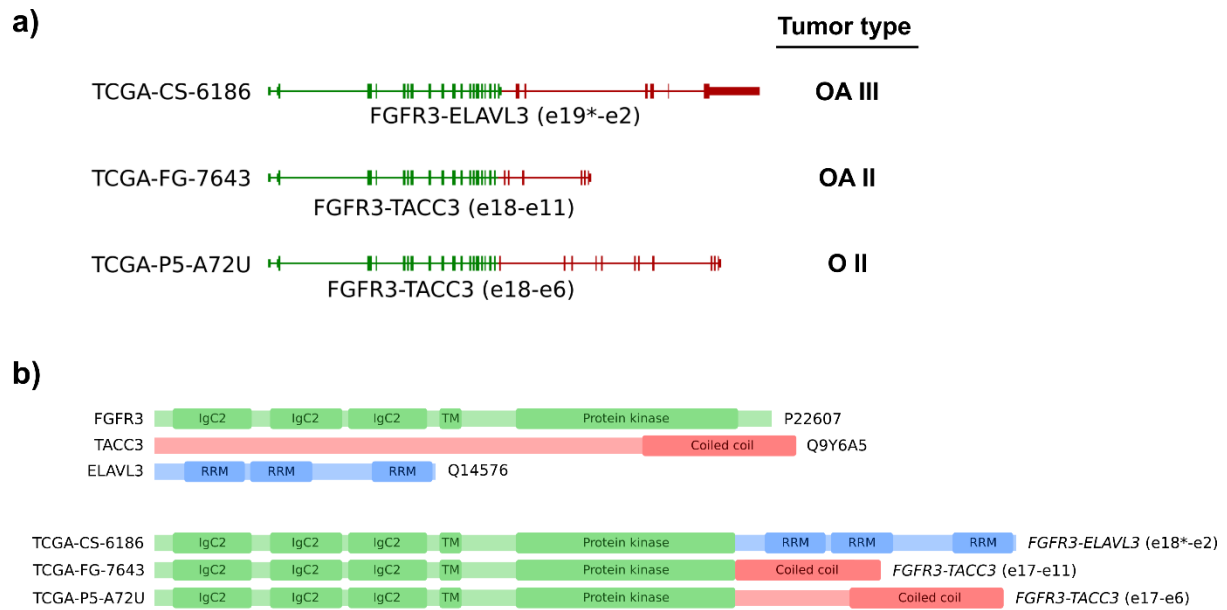

Supplementary Figure 7. Cause-specific survival rate did not significantly differ between cases with different FGFR3 immunostaining intensities within a) IDH1 p.R132H negative grade II-IV tumors (p = 0.119, n = 370, log-rank test), b) IDH1 p.R132H negative glioblastomas (grade IV) (p = 0.525, n = 343, log-rank test) or c) all the glioblastomas (grade IV) (p = 0.203, n = 414, log-rank test). IDH1 mutation status was evaluated using immunohistochemistry.
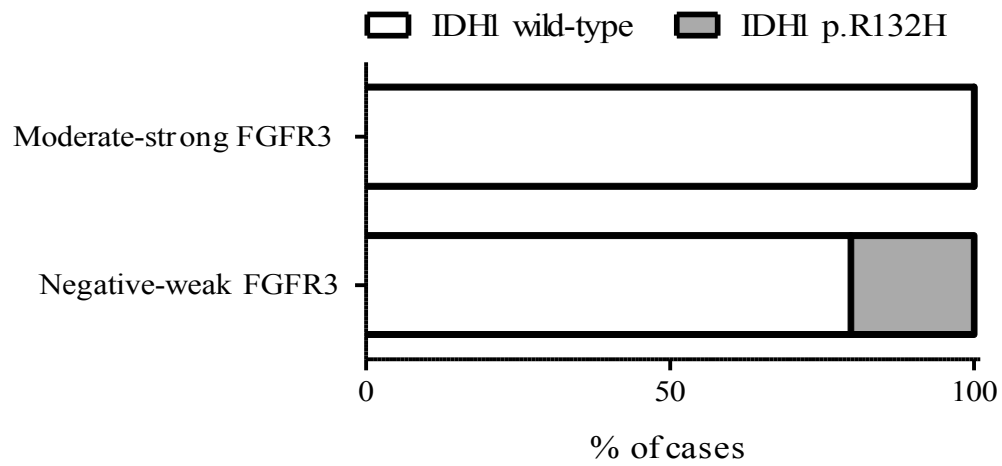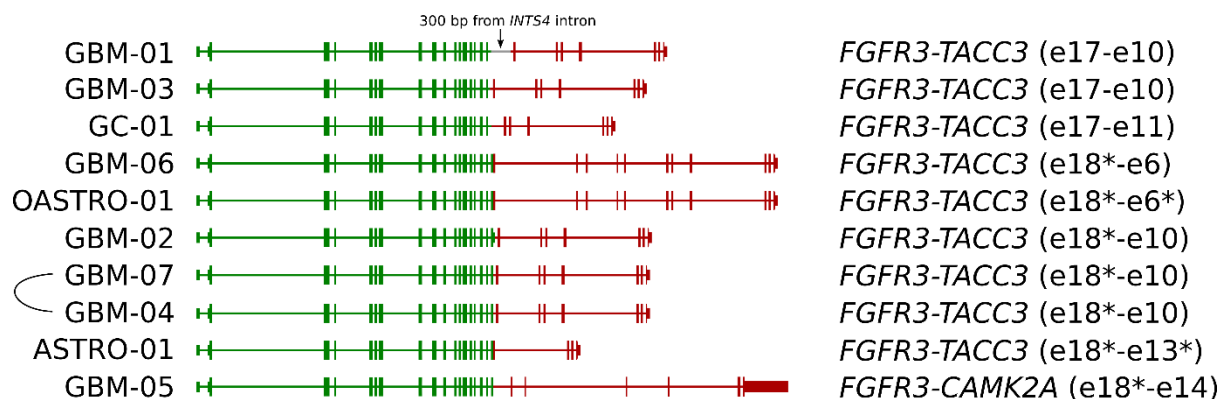
Supplementary Figure 8. Moderate-to-strong FGFR3 staining was observed only in cases that lack p.R132H mutation (p > 0.05, Fisher's exact test). Only primary astrocytic tumors were included into the analysis.

Supplementary Figure 9. Representative images (100x magnification) from three cases (ASTRO-05, OLIGO-01, and GBM-11) with moderate FGFR3 staining and IDH1 p.R132H mutation. Staining is characterized by a membrane localization pattern. Scale bar 25 μm.

a)

TCGA-CS-6186 — FGFR3-ELAVL3 (e19*-e2) — OA III

TCGA-FG-7643 — FGFR3-TACC3 (e18-e11) — OA II

TCGA-P5-A72U — FGFR3-TACC3 (e18-e6) — O II

Tumor type

b)

FGFR3 — IgC2 IgC2 IgC2 TM Protein kinase — P22607
TACC3 — Coiled coil — Q9Y6A5
ELAVL3 — RRM RRM RRM — Q14576

TCGA-CS-6186 — IgC2 IgC2 IgC2 TM Protein kinase RRM RRM RRM — FGFR3-ELAVL3 (e18*-e2)
TCGA-FG-7643 — IgC2 IgC2 IgC2 TM Protein kinase Coiled coil — FGFR3-TACC3 (e17-e11)
TCGA-P5-A72U — IgC2 IgC2 IgC2 TM Protein kinase Coiled coil — FGFR3-TACC3 (e17-e6)

c)

negative   FGFR3 fusion

IDH negative   n=117

0   20   40   60   80   100

% of cases

Supplementary Figure 10. FGFR3 gene fusions detected in TCGA low-grade glioma cohort by using our own fusion detection algorithm on the transcriptome sequencing data (n = 467) (1). a) Transcript structures of FGFR3 gene fusions. Initial tumor type of each FGFR3 fusion positive case is marked next to the figure. O II: grade II oligoastrocytoma, OA II: grade II oligoastrocytoma, OA III: grade III anaplastic oligoastrocytoma b) Predicted protein structures of FGFR3 fusion genes detected in TCGA low-grade glioma cohort. c) The frequency of FGFR3 fusions in IDH wild-type low-grade gliomas (2.6%, n = 117) was similar to their frequency in GBM (2,3). No fusions were detected in IDH-mutated tumors.


300 bp from *INTS4* intron

GBM-01 — FGFR3-TACC3 (e17-e10)
GBM-03 — FGFR3-TACC3 (e17-e10)
GC-01 — FGFR3-TACC3 (e17-e11)
GBM-06 — FGFR3-TACC3 (e18*-e6)
OASTRO-01 — FGFR3-TACC3 (e18*-e6*)
GBM-02 — FGFR3-TACC3 (e18*-e10)
GBM-07 — FGFR3-TACC3 (e18*-e10)
GBM-04 — FGFR3-TACC3 (e18*-e10)
ASTRO-01 — FGFR3-TACC3 (e18*-e13*)
GBM-05 — FGFR3-CAMK2A (e18*-e14)

Supplementary Figure 11. Predicted transcript structures of FGFR3 fusion genes detected in our targeted sequencing cohort and in TCGA low-grade glioma cohort.
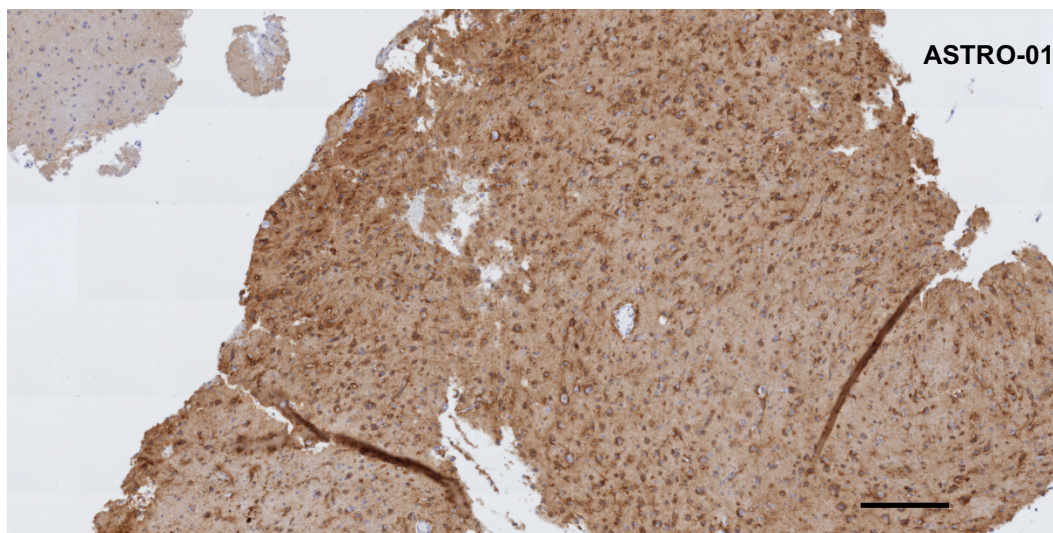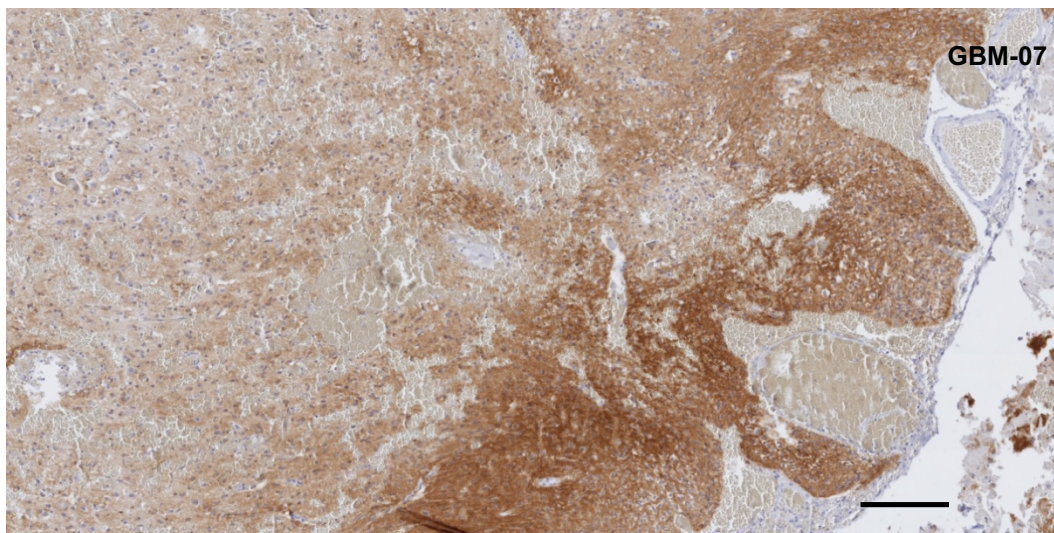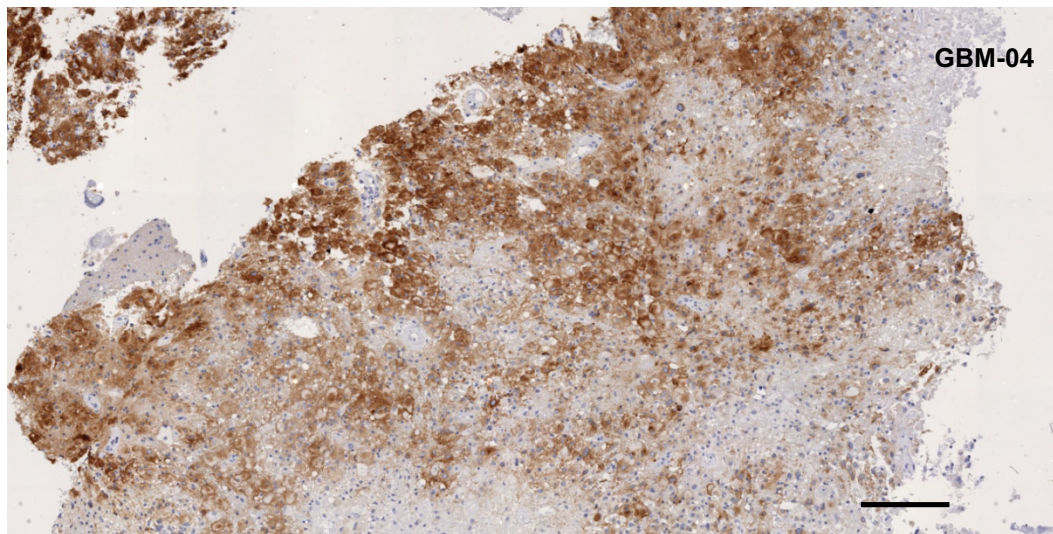
a)

ASTRO-02

OASTRO-02
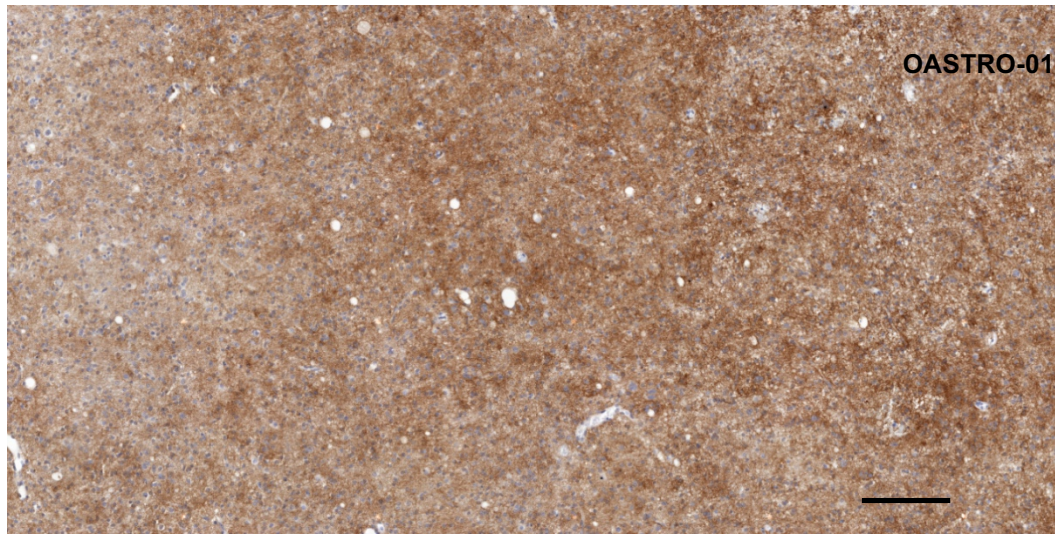
b)

GBM-03

GBM-04

GBM-07
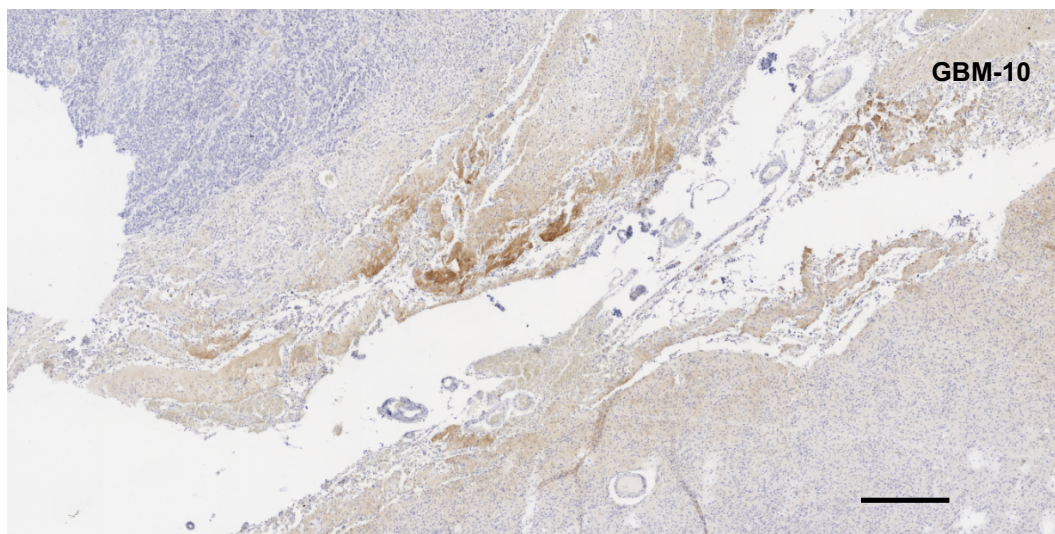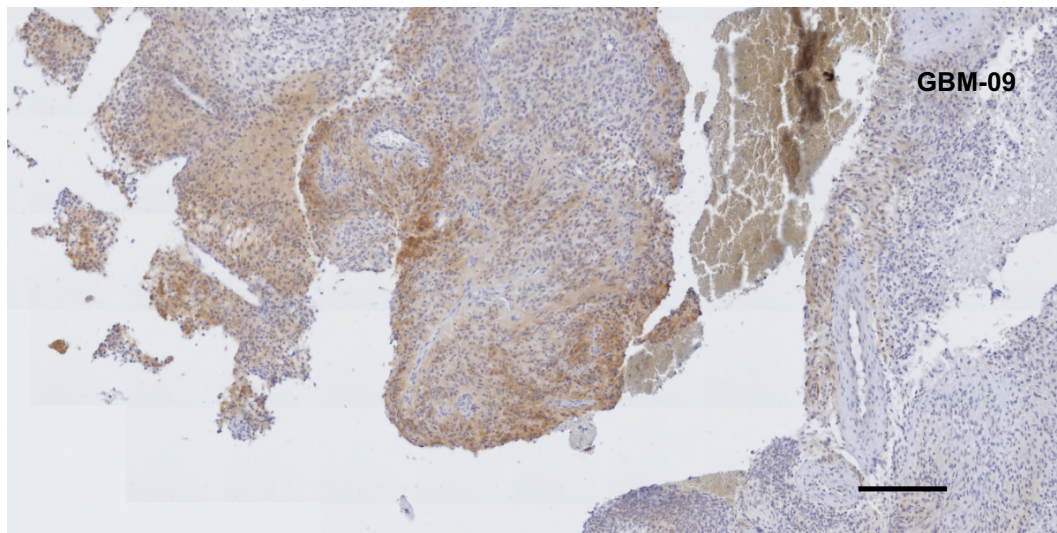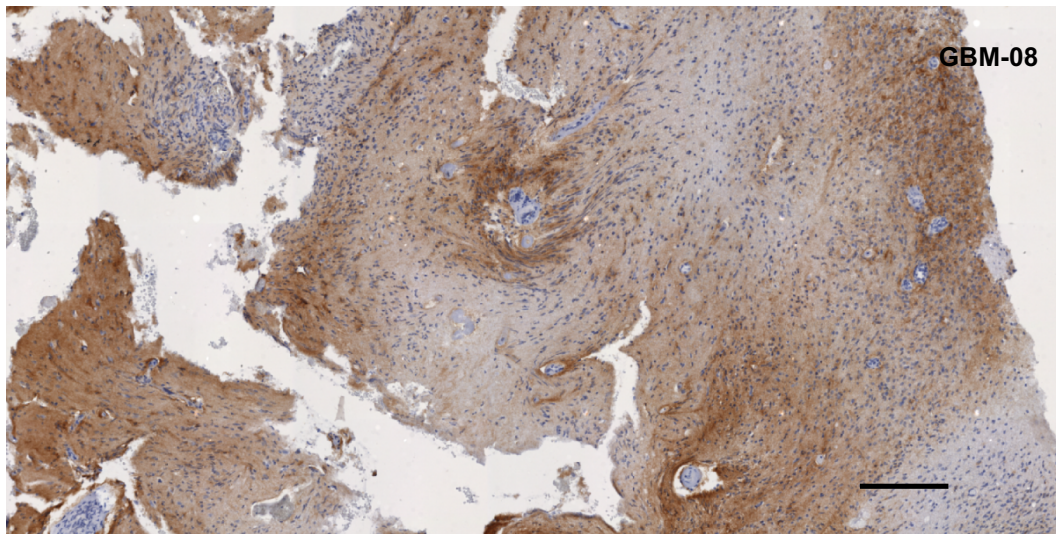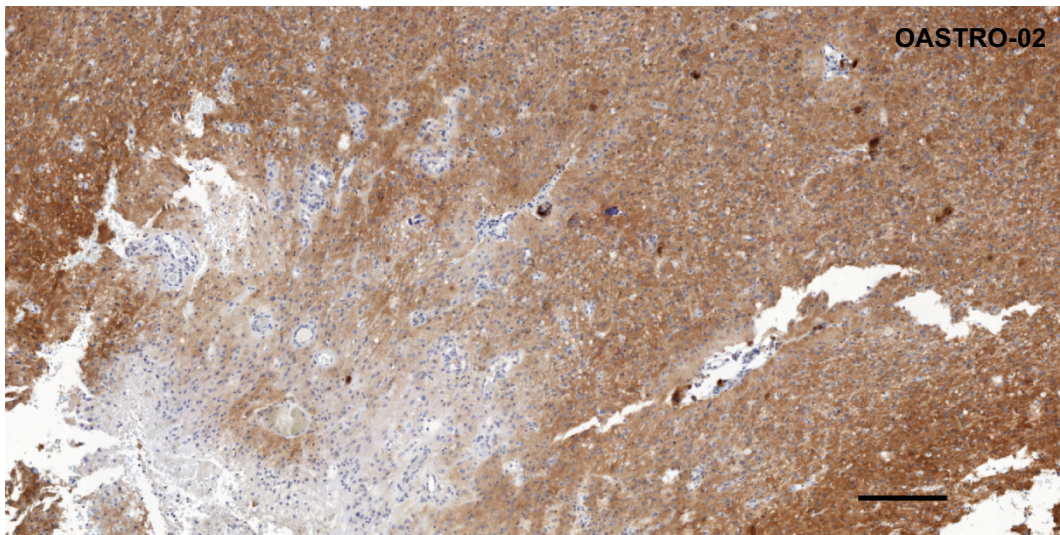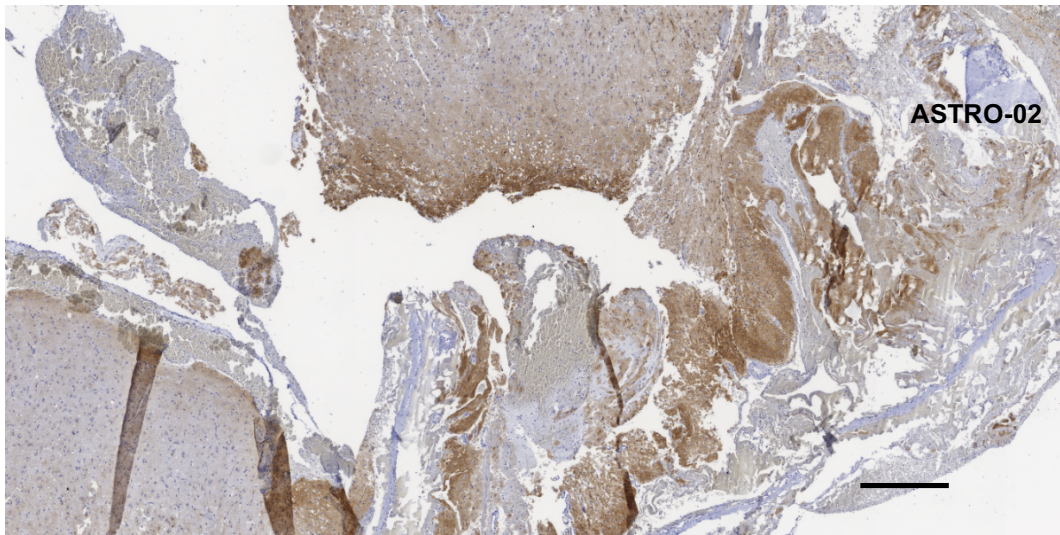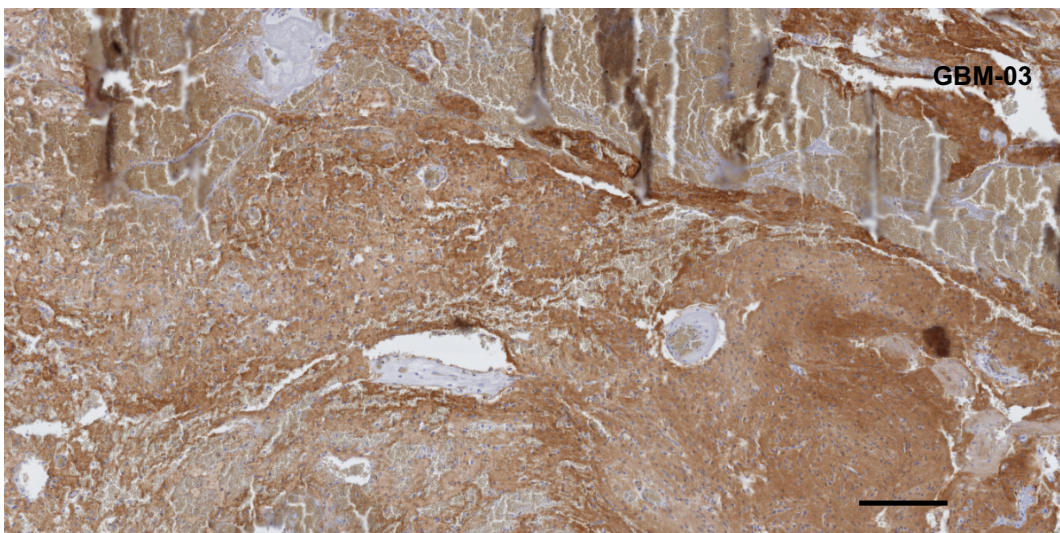
ASTRO-01

Supplementary Figure 12. a) Representative images (50x magnification) from five cases (GBM-08, GBM-09, GBM-10, ASTRO-02, and OASTRO-02) with strong FGFR3 staining but lacking validated intergenic rearrangements. Strong FGFR3 staining was rather focal in GBM-09, GBM-10, and ASTRO-02. Edge staining artefact can be also seen in the ASTRO-02 image. b) Representative images (50x magnification) from five FGFR3 fusion-positive cases (GBM-03, GBM-04, GBM-07, ASTRO-01, and OASTRO-01). Scale bar 50 µm. Representative images of GBM-01, GBM-05, and GBM-06 are shown in Figure 3.
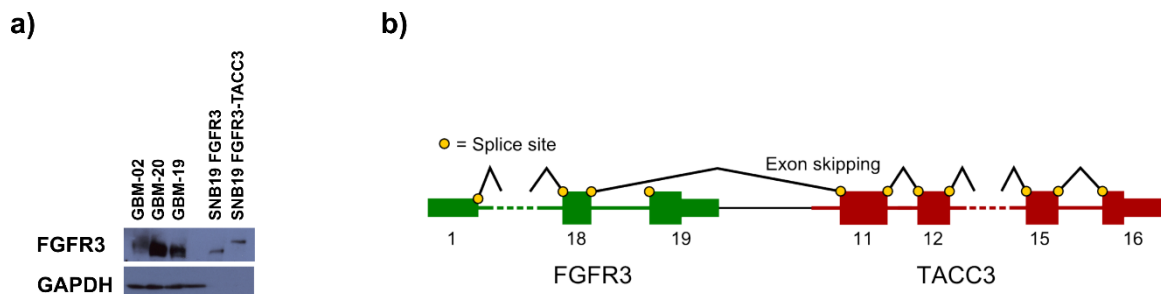

Supplementary Figure 13. a) Fusion protein is expressed in sample GBM-02. FGFR3 and fusion protein levels were detected with Western blotting. Elevated molecular weight is observed in sample GBM-02 and SNB19 cells overexpressing FGFR3-TACC3 fusion. FGFR3 fusions were not detected in GBM-20 or GBM-19. SNB19 cells overexpressing wild-type FGFR3 were also used as a control. b) Last exon of FGFR3 is removed during splicing, as splicing acceptor site is not present in that exon. The figure modified from (3).

a)

b)

c)

d)


e)

Supplementary Figure 14. FGFR3-staining was efficiently diminished when either a) full length epitope or b) one of 25 amino acid long fragments from the epitope region was used as a blocking peptide during the immunohistochemical staining. c) FGFR3 control staining from the same region. Staining was performed without any blocking peptide. d) Only red blood cell and hemosiderin staining was apparent, when 25 amino acid long blocking peptide was used. e) FGFR3 control staining from the same region. Staining was performed without any blocking peptide. All the images are with 100x magnification. Scale bar 100 µm.
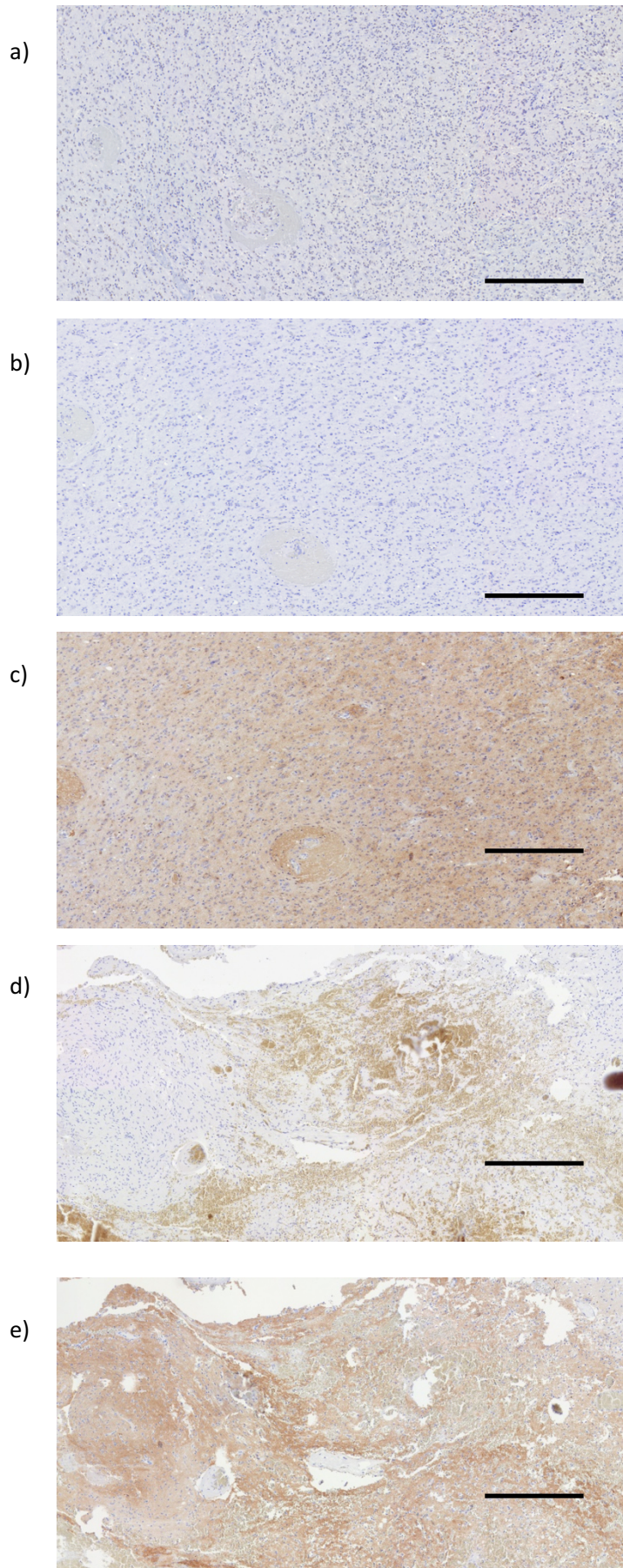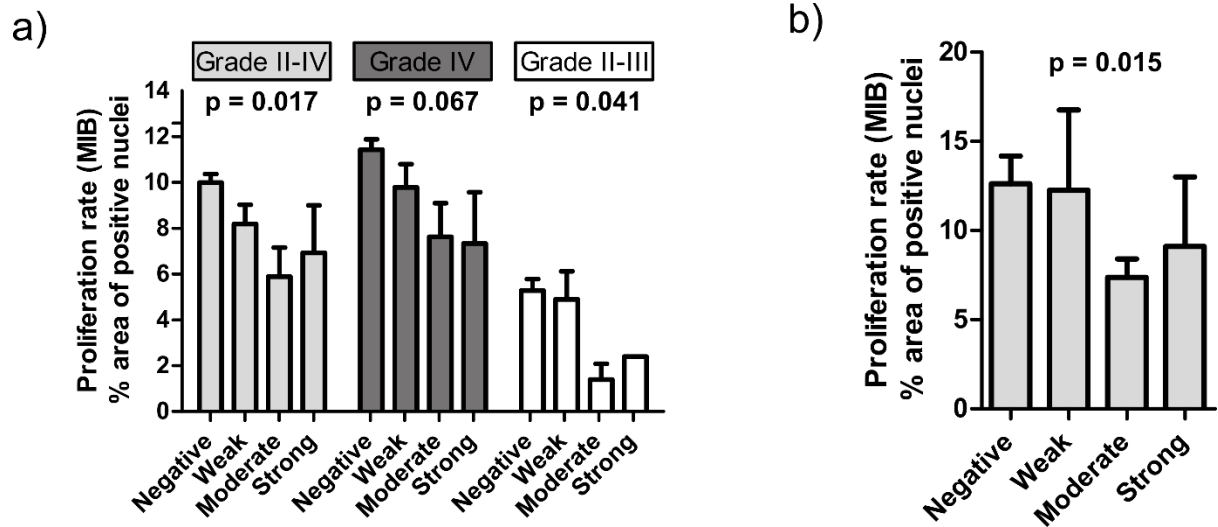
Supplementary Figure 15. Tumors with moderate-to-strong FGFR3 staining showed a lower proliferation rate than did negatively-to-weakly stained tumors both in the astrocytoma TMA cohort (a) and among glioblastoma samples used for whole-mount tissue staining (b). The mean proliferation rate and SEM are shown. Statistical significance was calculated using Kruskal-Wallis Test.

Supplementary Figure 16. FGFR3-fusion status and FGFR3 IHC staining intensity were not associated with patient prognosis in glioblastoma cohort used for whole-mount tissue staining. Only primary cases were included into the analysis.
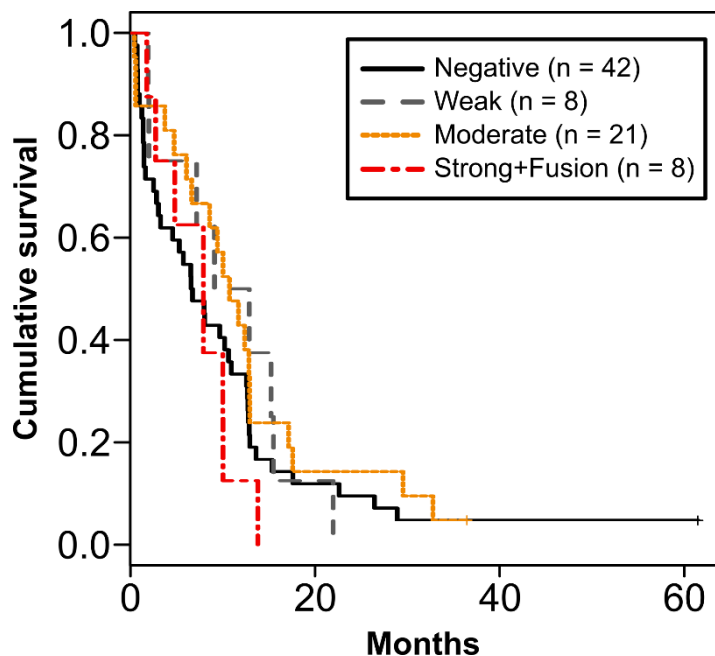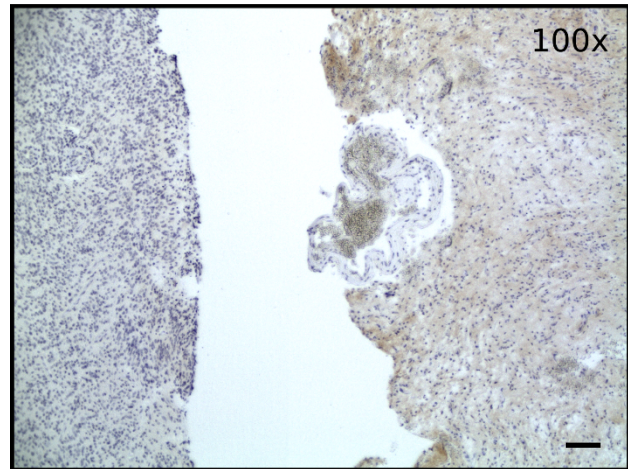
Supplementary Figure 17. A representative staining image showing stronger FGFR3 staining in less cellular tumor area. Scale bar 40 μm.

REFERENCES

(1) Cancer Genome Atlas Research Network. Comprehensive, Integrative Genomic Analysis of Diffuse Lower-Grade Gliomas. N Engl J Med [Internet]. 2015; Available from: http://dx.doi.org/10.1056/NEJMoa1402121

(2) Brennan CW, Verhaak RGW, McKenna A, Campos B, Noushmehr H, Salama SR, et al. The somatic genomic landscape of glioblastoma. Cell. 2013;155:462–77.

(3) Parker BC, Annala MJ, Cogdell DE, Granberg KJ, Sun Y, Ji P, et al. The tumorigenic FGFR3-TACC3 gene fusion escapes miR-99a regulation in glioblastoma. J Clin Invest. 2013;123:855–65.